3D Surface Simplification Based on Extended Shape Operator

JUIN-LING TSENG, YU-HSUAN LIN
Department of Computer Science and Information Engineering, Department and Institute of Electrical Engineering
Minghsin University of Science and Technology
No.1, Hsin Hsin Road, Hsin Feng, Hsin Chu County
TAIWAN
flysun@must.edu.tw (corresponding author), aurora0715@gmail.com

Abstract: - In order to present realistic scenes and models, complex triangle meshes comprising large numbers of triangles are often used to describe 3D models. However, with an increase in the number of triangles, storage and computation costs will raise. To preserve more geometric features of 3D models, Zhanhong and Shutian employed the curvature factor of collapsing edge, Gaussian Curvature, to improve the Quadric Error Metrics (QEM) simplification. Their method allows the QEM not only to measure distance error but also to reflect geometric variations of local surface. However, the method can only estimate the curvature factors of vertices in manifold surfaces due to Gaussian Curvature. To overcome this problem, we propose a new simplification method, called Extended Shape Operator. The Extended Shape Operator estimates the local surface variation using three-rings shape operator. The Extended Shape Operator can be applied in the simplification of manifold and non-manifold surfaces. In our experiment, we employed the error detection tool, Metro, to compare errors resulting from simplification. The results of the experiment demonstrate that when the model has been simplified, the proposed method is superior to the simplification method proposed by Zhanhong and Shutian.

Key-Words: - surface simplification, extended shape operator, curvature factor, quadric error metric

1 Introduction

The increased prevalence of information devices in recent years has increased the use of 3D modeling [14, 15, 16, 17]. Many 3D models comprise hundreds of thousands or even millions of triangles; for mobile devices, processing the large quantities of data in these models may affect the execution speed of programs or games, and therefore, the most direct solution is to reduce the number of triangles used to describe the 3D model, the process of which is called surface simplification [3, 4].

The ultimate objective of surface simplification in 3D models is to reduce the number of triangles in the model without reducing the quality [5, 6, 12]. In addition, the characteristic contours of the model must also be taken into consideration during the process of simplification to avoid excessive damage to the resulting contours. Many simplification methods have been proposed [2, 13], including vertex decimation [10], vertex clustering [9], edge contraction [7], triangle contraction [8], and quadric error metrics simplification [1]. Among these approaches, Quadric Error Metrics (QEM) simplification is considered the closest to optimal.

The Curvature Factor [14] is based on the QEM simplification. This method used Gaussian Curvature to define the concept of curvature factors of collapsing edge and embed it into the original QEM proposed by Garland. This method can prevent more geometric features than original QEM. However, only the vertices of the full disc in the manifold meshes can this method estimate, shown in Fig.1.

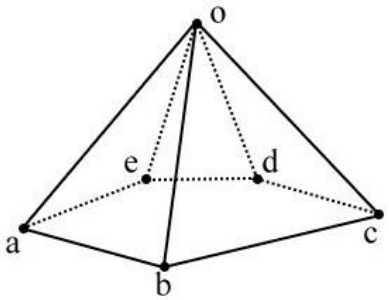

Fig. 1: Full disc in manifold mesh

According to the definition of Chen et al.[18], a surface is a manifold if each point has a neighborhood homeomorphic to a disc in the real plane. They take some examples of common mesh structures that are incompatible with the manifold definition are shown in Fig. 2.

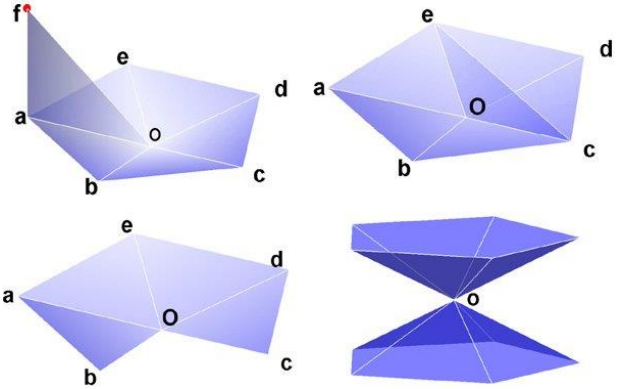

Fig. 2: Some examples of non-manifold meshes [18]

In fact, QEM simplification also supports non-manifold surface models besides manifold ones. Although the curvature factor [14] is based on the QEM simplification, it cannot be used to calculate the curvature factors of the vertices in non-manifold meshes, even the boundary vertices.

To overcome this problem, we proposed a new curvature estimation method, called Extended Shape Operator (ESO). The ESO estimates the curvature factors using the shape operators between the vertex and its neighbor vertices. Additionally, the ESO also extends the size of estimation from 1-ring neighborhood of the Curvature Factor to three rings. Experimental results show the ESO can not only keep the geometric features but also decrease more errors caused by simplification.

2 Related Work

2.1 Quadric Error Metrics Simplification

This method involves contracting vertex v_1 and vertex v_2 into a new vertex, v_p, the location of which is obtained using the distance values of a vertex and the conjoining triangles. The minimum distance value determines the location of the new vertex v_p. The estimated distance value also represents the resulting error of simplification. In this manner, the QEM simplification moderately maintains the outer shape of the model while reducing the number of triangles within, thereby reducing the resulting errors. The estimated position of v_p also strongly influences changes in the surrounding triangles (Fig. 3).

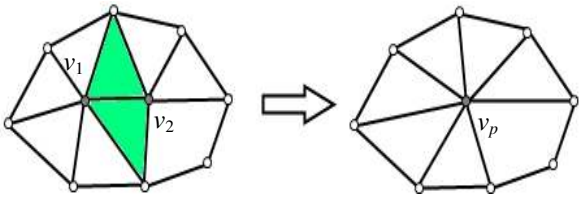

Fig. 3: Quadric Error Metrics Simplification

In a three-dimensional space, suppose the equation of plane p is $ax+by+cz+d=0$, where $a^2+b^2+c^2=1$. The distance between this plane and any vertex $v=[v_x\ v_y\ v_z\ 1]^T$ is thus as shown in Eq. (1): [1]

$$D_p^2(v)=(p^Tv)^2=v^T(pp^T)=v^TK_pv \tag{1}$$

Garland used quadric error metrics for the measurement of error in model simplification, defining error as:

$$Error(v)=v^TK_pv \tag{2}$$

where K_p can be expressed as:

$$K_p=p\cdot p^T=\begin{bmatrix}a\\b\\c\\d\end{bmatrix}\cdot\begin{bmatrix}a & b & c & d\end{bmatrix}=\begin{bmatrix}a^2 & ab & ac & ad\\ ab & b^2 & bc & bd\\ ac & bc & c^2 & cd\\ ad & bd & cd & d^2\end{bmatrix} \tag{3}$$

In the application of K_p to measure surface error in QEM simplification, the error that each qualifying vertex pair may potentially cause after simplification must be estimated; simplification is then applied to the vertex pairs that will result in the least error. In this way, excessive damage can be prevented and the contour of the object can be preserved. In addition, this action is repeatable for surface simplification.

The main advantage of this simplification method is fast and keeps low average error. However, this method considered only its distance metric, it is not suitable for simplifying models with sharp angles. To solve this problem, Zhanhong and Shutian proposed the Curvature Factor method to reserve quite a number of important shape features and reduce visual distortion effectively. [14]

2.2 Curvature Factor

In order to preserve the sharp features after simplifying, Zhanhong and Shutian defined an edge curvature factor. This factor is estimated by the Gaussian Curvature proposed by Meyer et al., the Gaussian Curvature formula as follow [19]:

$$K_{v_i}=\frac{1}{A(v_i)}\left(2\pi-\sum_j^{\#f}\theta_j\right) \tag{4}$$

where $A(v_i)$ presents the area sum of adjacent triangle of v_i, θ_j is the angle of the j-th face at the vertex v_i, and $\#f$ denotes the number of faces around this vertex.

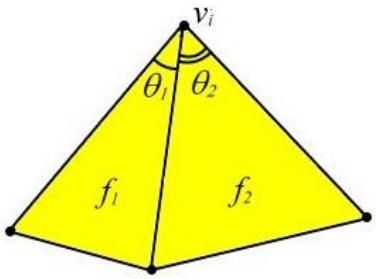

Fig. 4: Estimation of the Gaussian Curvature of v_i

The edge curvature factor is defined as follow:

$$K = \frac{\left|2\pi - \sum_j^{\#f_{v1}} \theta_j\right| + \left|2\pi - \sum_k^{\#f_{v2}} \theta_k\right|}{A(v_1) + A(v_2)} \quad (5)$$

where v_1 and v_2 are the vertices of an edge, $A(v_1)$ and $A(v_2)$ present the area sum of adjacent triangle of v_1 *and* v_2 respectively, θ_j is the angle of the j-th face at the vertex v_1, θ_k is the angle of the k-th face at the vertex v_2, and $\#f_{v1}$ and $\#f_{v2}$ denote the number of faces around v_1 and v_2 respectively.

The edge curvature factor used the Gaussian Curvature to improve the quadric error metrics and kept more sharp features. The latter can simplify the manifold and non-manifold meshes, but the former is only suitable to be applied to the manifold ones.

If the edge curvature factor is used to simplify the non-manifold meshes, the Eq.5 could not find out suitable curvature values. The examples that are unsuitable to use the Eq.5 are as follows:

1. An edge meeting the estimated vertex is shared by three triangles:

   Every edge in a manifold mesh should be shared by only two triangles. Therefore, if an edge meeting the estimated vertex is shared by three triangles, the angle sum of all faces at the estimated vertex would be more than 2π, as shown in Fig.5. That is, the estimation of Gaussian Curvature value would be minus if the surface the estimated vertex lies on is an even one. This value would present the surface variation incorrectly.

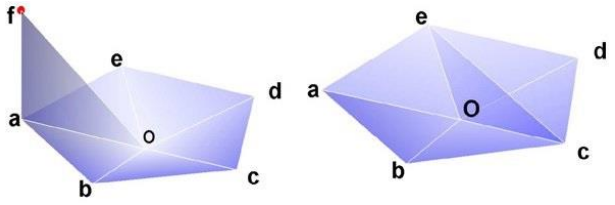

Fig. 5: An edge meeting the estimated vertex *o* is shared by three triangles [18]

2. Boundary vertex:

   When the estimated vertex is a boundary vertex, some edges will have only one incident triangle. That is, the angle sum of all faces at the estimated vertex would be far less than 2π, even though the surface that the estimated vertex lies on is an even one. This case will take low-curvature surfaces for high-curvature surfaces.

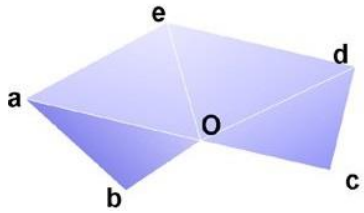

Fig. 6: The estimated vertex *o* is a boundary vertex [18]

3. There are two incident cones on the estimated vertex:

   According to the definition of manifold surfaces, each vertex should have only one incident cone. Therefore, if there are two incident cones on the same estimated vertex, the angle sum of all faces at the estimated vertex would be far more than 2π, even up to 4π. This case will impact the determination of the edge curvature factor when collapsing edge.

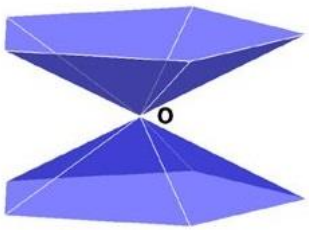

Fig. 7: There are two incident cones on the estimated vertex *o* [18]

To overcome these problems, we propose a new simplification method, called Extended Shape Operator. Our method can not only estimation surface variation on non-manifold meshes, but also decrease more errors caused by simplification than the one proposed by Zhanhong and Shutian.

3 Shape Operator

Suppose p is a point on surface M, and v is the tangent vector to M at p. The shape operator for tangent vector v at p can thus be defined as $S_p(v)$:

$$S_p(v) = -\nabla_v U \quad (6)$$

where U is the normal vector field in the neighborhood of p on M (Fig. 8); the shape operator $S_p(v)$ represents the variation in normal vector U at p on M in the direction of v (Fig. 9).

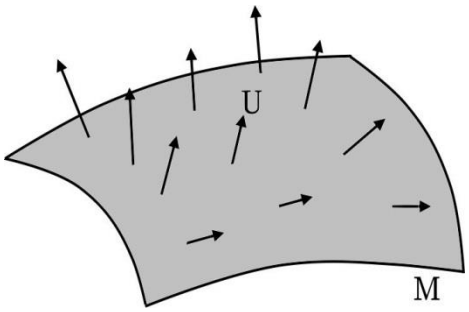

Fig. 8: Normal vector field on surface M [2]

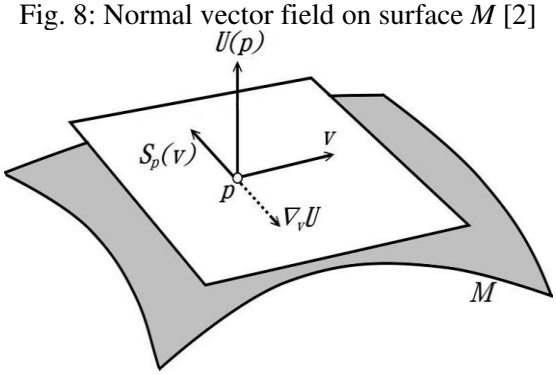

Fig. 9: Shape operator estimation for tangent vector v at point p on surface M [2]

The shape operator refers to the variation in the normal vector field in the direction of vector v at point p on surface M. To calculate surface changes in the neighborhood of p, Jong et al. [2, 13] used variations in the normal vectors of p and its neighboring points for estimation. Suppose the k neighboring points of p are p_1, p_2, p_3,…, and p_k, and the tangent vectors of p toward each neighboring point are t_1, t_2, t_3,…, and t_k . Calculations from Eq. 6 provide the shape operators $S_p(t_1)$, $S_p(t_2)$, $S_p(t_3)$,…, and $S_p(t_k)$ at p in the directions of t_1, t_2, t_3,…, and t_k. Integrating all of the shape operators enables the derivation of the following formula to estimate variations in the surface surrounding p:

$$S_p = \frac{\sum_{i=1}^{k} \|U(p_i) - U(p)\|}{\sum_{i=1}^{k} \|p_i - p\|} \qquad (7)$$

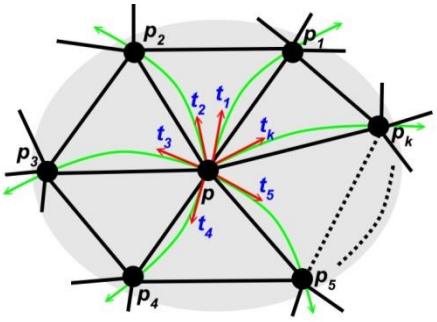

Fig. 10: Shape operators of point p using the tangent vectors to each neighboring point to estimate local surface variation

In practice, this is based on a tangent plane. Suppose there is a tangent plane TP_p at point p; the projections of $\overrightarrow{pp_1}$, $\overrightarrow{pp_2}$, $\overrightarrow{pp_3}$,…, and $\overrightarrow{pp_k}$ are used to obtain the required tangent vectors t_1, t_2, t_3,…, and t_k, which are then employed to derive the shape operators at p in the direction of said vectors. Using the shape operators enables the estimation of overall variations in the local surface area. Examples of implementation results are presented in Fig. 11.

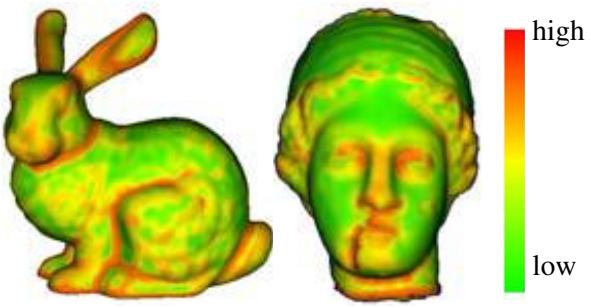

Fig. 11: Surface variation estimation; green represents areas of minor variation, whereas red indicates areas of major variation

The shape operator is used to estimate surface variations by neighboring vertices on 3D models prior to vertex-pair contraction in order to reduce the error caused by simplification. Nevertheless, for the simplification of models at lower resolutions, considering only the first ring of neighboring vertices is far from adequate. When simplification results in a smaller number of triangles, the simplified vertices cover a larger area. For this reason, the range under consideration should also be extended. This study proposes the Extended Shape Operator to reduce error resulting from the simplification to the fewest possible number of triangles.

4 Extended Shape Operator

4.1 Analyzing the Impact Area of Simplified Vertices

To analyze the impact areas of simplified vertices, we perform an experiment to calculate the moving distance of each simplified vertex. This experiment uses four models, including a cow, a dragon, a femur and an isis. The half edge collapse [1] is adopted to record the moving path of each simplified vertex in the simplification process because it will allow the vertex moving to the other one in the collapsing edge.

In this experiment, we simplify the above models into five different resolutions, include 40%, 30%, 20%, 10% and 5%. The experimental results are shown in Tables 1 to 4. In these tables, the moving length presents the moving times of vertex when it is simplified. Taking the cow model (Table 1) as an example, when the cow model is simplified into forty percent of triangles, 1315 vertices are moved one time, 387 vertices are moved two times, 38 vertices are move three times, 2 vertices are moved more than 3 times, and 1162 vertices still stay at their original positions.

Table 1: Moving length analysis of simplified vertex (cow model; the number of vertices =2904)

SP	5%	10%	20%	30%	40%
ML	The number of vertices				
0	148	293	583	873	1162
1	651	971	1272	1359	1315
2	1021	1025	810	566	387
3	726	490	218	102	38
>3	358	125	21	4	2
AML	2.19	1.72	1.25	0.97	0.76

SP : simplification percentage
ML : moving length
AML : average moving length

Table 2: Moving length analysis of simplified vertex (dragon model; the number of vertices=25418)

SP	5%	10%	20%	30%	40%
ML	The number of vertices				
0	1277	2546	5084	7622	10160
1	6095	9147	12308	13320	12906
2	9691	9617	6862	4026	2036
3	6327	3501	922	226	92
>3	2028	607	242	224	224
AML	2.11	1.66	1.21	0.94	0.75

Table 3: Moving length analysis of simplified vertex (femur model; the number of vertices=76794)

SP	5%	10%	20%	30%	40%
ML	The number of vertices				
0	3873	7715	15397	23074	30748
1	17366	26040	34774	37525	36496
2	28309	29082	22278	14739	9025
3	20201	12088	4108	1421	519
>3	7045	1869	237	35	6
AML	2.13	1.67	1.21	0.93	0.73

Table 4: Moving length analysis of simplified vertex (isis model; the number of vertices=100002)

SP	5%	10%	20%	30%	40%
ML	The number of vertices				
0	5002	10002	20002	30002	40002
1	23494	35670	48645	52994	51925
2	38204	38757	27985	16393	7990
3	25715	14100	3322	612	85
>3	7587	1473	48	1	0
AML	2.08	1.61	1.15	0.88	0.68

According to the experimental results, the average moving lengths are less than three, even if the models are simplified into only five percent of the number of triangles. Additionally, the percent of the number of vertices that the moving lengths are less than or equal three are almost over ninety percent, as shown in Table 5. Therefore, we extend the range from one ring to three rings for the estimation of surface variation.

Table 5: The percent of the number of vertices with moving length<=3 in different simplification percentage

SP	5%	10%	20%	30%	40%
Models	The percent of the number of vertices with moving length<=3 (%)				
cow	87.67	95.70	99.28	99.86	99.93
dragon	92.02	97.61	99.05	99.12	99.12
femur	90.83	97.57	99.69	99.95	99.99
isis	92.41	98.53	99.95	100	100

SP: simplification percentage

4.2 The Proposed Algorithm

Shape operators generally only consider the neighboring points of p, as shown in Fig. 12(a). To obtain a low-resolution model of higher quality after simplification, this study expanded the estimation range to N rings of neighboring points. As shown in Fig. 12(b), $p_{1,1}$, $p_{1,2}$, $p_{1,3}$,…, and p_{1,M_1} represent the first ring of points neighboring p; $p_{2,1}$, $p_{2,2}$, $p_{2,3}$,…, and p_{2,M_2} are the second ring of points neighboring p, and $p_{3,1}$, $p_{3,2}$, $p_{3,3}$,…, and p_{3,M_3} comprise the third ring of points neighboring p. Likewise, we can define the Nth ring of points neighboring p as $p_{N,1}$, $p_{N,2}$, $p_{N,3}$,…, and p_{N,M_N}. As simplification of the

model proceeds, the number of triangles in the mesh of the model dwindles. In other words, the impact range of each vertex expands and the data that each vertex encompasses increases as well. For example, as shown in Fig. 13, point p is a vertex on a dragon model; during the first simplification, the area that p influences lies within the first ring of neighboring points. During the second simplification, the area that p may influence extends to the second ring of neighboring points, and so forth. After several iterations, the area influenced by each vertex expands. Therefore, we extended the estimation range of the shape operator to the Nth ring. The formula to estimate the N-rings shape operator of the area where p is located is:

$$S_p^N = \frac{\sum_{j=1}^{N}\sum_{i=1}^{M_j}\left(\left\|U(p_{j,i})-U(p)\right\|\right)}{\sum_{j=1}^{N}\sum_{i=1}^{M_j}\left\|p_{j,i}-p\right\|} \qquad (8)$$

where

N : the number of rings;
$p_{j,i}$: the ith point neighboring p in the jth ring;
$U(p_{j,i})$: the normal vector at point $p_{j,i}$;
M_j: the number of points neighboring p in the jth ring.

The variations in the normal vectors of each ring are:

The first ring : $\sum_{i=1}^{M_1}\left(\left\|U(p_{1,i})-U(p)\right\|\right)$
The second ring : $\sum_{i=1}^{M_2}\left(\left\|U(p_{2,i})-U(p)\right\|\right)$
The third ring : $\sum_{i=1}^{M_3}\left(\left\|U(p_{3,i})-U(p)\right\|\right)$
:
:
:
The Nth ring : $\sum_{i=1}^{M_N}\left(\left\|U(p_{N,i})-U(p)\right\|\right)$

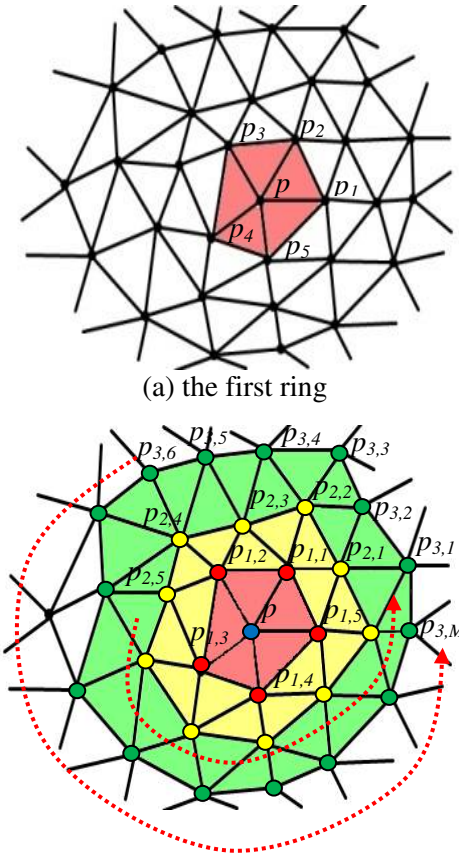

(a) the first ring

(b) the first to third rings

Fig. 12: N rings centered at p (N=1…3)

Basically, the Extended Shape Operator simplification is an improved algorithm for the QEM simplification. Prior to estimating the QEM, we first find out the N-rings shape operator S_p^N for each point p, calculate the surface variation within the range of N rings neighboring p, and then use S_p^N as the weight value to improve the QEM. The Extended Shape Operator can reduce the error caused by simplification when the model is simplified to lower resolutions.

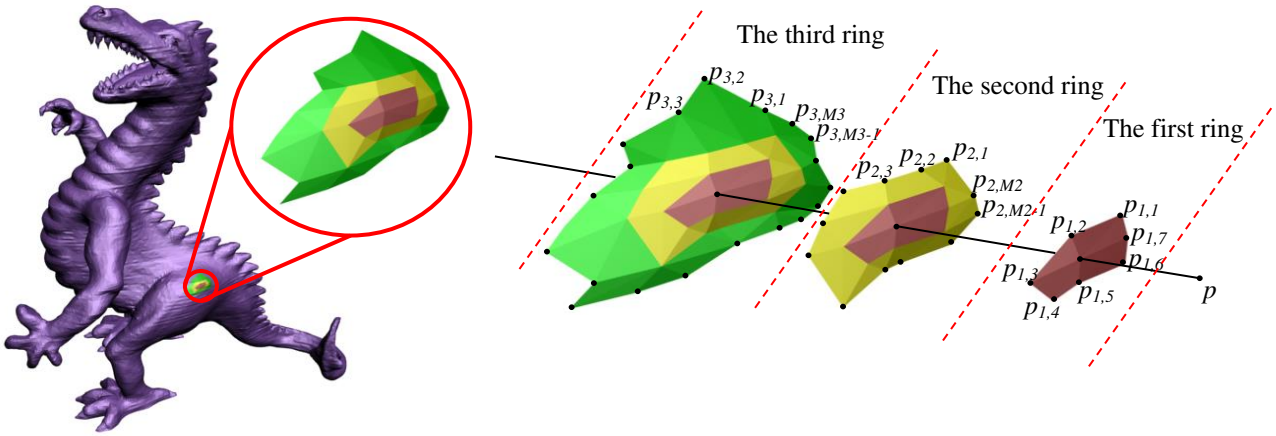

Fig. 13: The N-rings neighboring points of point p

The primary calculation steps of the proposed simplification approach are as follows:

1. Calculate the shape operator of each vertex $\{(p_{1,1}, p_{1,2},\ldots, p_{1,M1}), (p_{2,1}, p_{2,2},\ldots, p_{2,M2}),\ldots, (p_{N,1}, p_{N,2},\ldots, p_{N,MN})\}$. Using Eq. (8), estimate the N-rings shape operator S_p^N of p and change the QEM estimation formula to:
$$Q(p) = S_p^N \cdot \sum K_f \qquad (9)$$
where
f is the plane encompassing the triangles with p as a vertex;
K_f represents the 4×4 matrix of plane f.
2. Select each qualifying vertex pair (v_1,v_2), and calculate the minimum error resulting from simplification.
3. Select the vertex pair (v_1,v_2) with the minimum error for simplification.
4. Contract vertex pair (v_1,v_2) into $\bar{v}$, and calculate the QEM of $\bar{v}$ using $Q=(Q_1+Q_2)$, where Q_1 and Q_2 are the QEMs of v_1 and v_2 , respectively.
5. Update the information regarding the points neighboring v_1 and v_2.
6. Repeat the steps above until the designated number of triangles is reached.

5 Experimental Results

This study implemented an experiment with three rings to verify the Extended Shape Operator (ESO) simplification method proposed in this study. We conducted comparisons with the Curvature Factor. Four models were employed for the simplification experiment: a cow, a dragon, a femur, and an isis. The number of vertices and triangles are shown in Table 6.

Table 6: Information of Experimental Models

Model	Vertices	Triangles
Cow	2904	5804
Dragon	25419	50761
Femur	76794	153322
Isis	100002	200000

This study employed Hausdorff Distance implemented in Metro [11] to measure the error caused by simplification and understand the variations in the shapes of the models before and after simplification. Errors occurring in the Curvature Factor (CF) [14] were also measured. The results of the four methods were then compared.

The results of the experiment show that the proposed method is more effective than the Curvature Factor method in reducing error. In the cow model, for example, the number of triangles was reduced from 5804 to 2321, 1741, 1160, 580 and 290. The Curvature Factor resulted in errors of 0.02146, 0.02552, 0.02985, 0.02948, and 0.04829, respectively, whereas the proposed method only caused errors of 0.00415, 0.00497, 0.00636, 0.01126, and 0.01813. This accounted for improvements of 80.68%, 80.53%, 78.71%, 61.81%, and 62.46% compared to the Curvature Factor, respectively, as shown in Table 7, Fig.14 and Fig.21.

Table 7: Hausdorff Distance Comparison (unit : 10^{-2}) – cow model

SP	Triangles	CF	ESO	IR
40%	2321	2.146	0.415	80.68%
30%	1741	2.552	0.497	80.53%
20%	1160	2.985	0.636	78.71%
10%	580	2.948	1.126	61.81%
5%	290	4.829	1.813	62.46%

SP : Simplification Percentage
IR : Improvement Rate

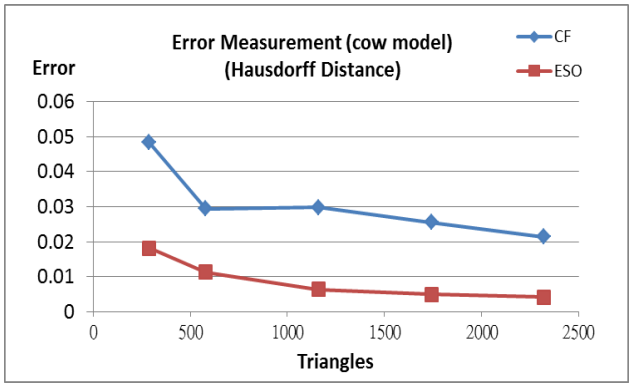

Fig. 14: Error measurement for cow model

Besides taking the cow model for verification, the dragon, femur and isis models are taken for experimental testing. In the dragon model, the original model contains 25419 vertices and 50761 triangles. Figure 22 shows the simplification results. Table 8 and Fig. 15 compare the error measurements with the Curvature Factor and the proposed method; the table shows that the proposed method can achieve an 45.95–81.08% error reduction. In the femur and isis models, the original models contain 153322 and 200000 triangles respectively. Figures 23 and 24 show the simplification results of the femur and isis models. Tables 9, 10 and Figs. 16, 17 compare the error measurements with the Curvature Factor and the

proposed method; the tables show that the proposed method can achieve 88.29–98.66% and 71.95–84.08% error reductions for the simplifications of the femur and isis models respectively.

Table 8: Hausdorff Distance Comparison (unit : 10^{-3}) – dragon model

SP	Triangles	CF	ESO	IR
40%	20304	2.622	0.496	81.08%
30%	15228	3.517	0.651	81.49%
20%	10152	4.055	1.002	75.29%
10%	5076	5.272	1.369	74.03%
5%	2538	5.384	2.910	45.95%

SP : Simplification Percentage
IR : Improvement Rate

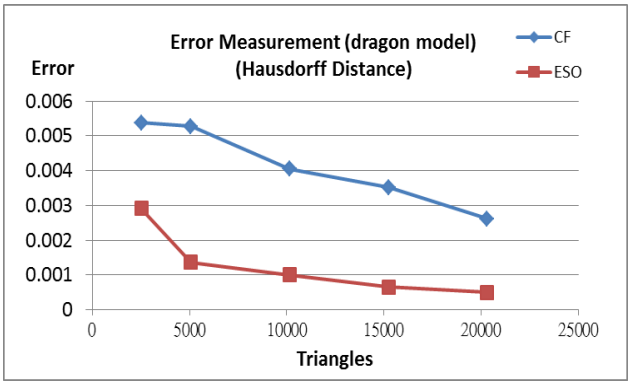

Fig. 15: Error measurement for dragon model

Table 9: Hausdorff Distance Comparison (unit : 10^{-3}) – femur model

SP	Triangles	CF	ESO	IR
40%	61328	17.206	0.231	98.66%
30%	45996	17.210	0.414	97.59%
20%	30664	17.264	0.649	96.24%
10%	15332	17.258	0.648	96.25%
5%	7666	17.202	2.015	88.29%

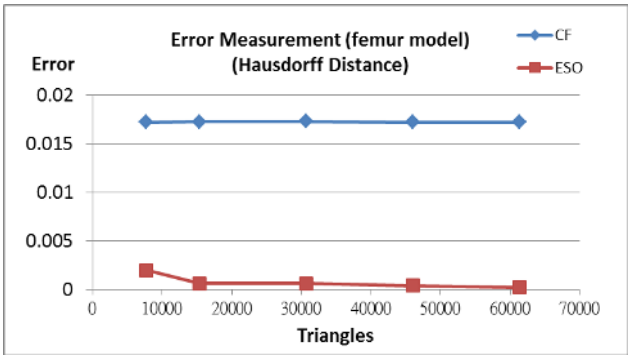

Fig. 16: Error measurement for femur model

Table 10: Hausdorff Distance Comparison (unit : 10^{-3}) –isis model

SP	Triangles	CF	ESO	IR
40%	80000	1.583	0.252	84.08%
30%	60000	1.986	0.408	79.46%
20%	40000	2.583	0.369	85.71%
10%	20000	2.830	0.683	75.87%
5%	10000	3.540	0.993	71.95%

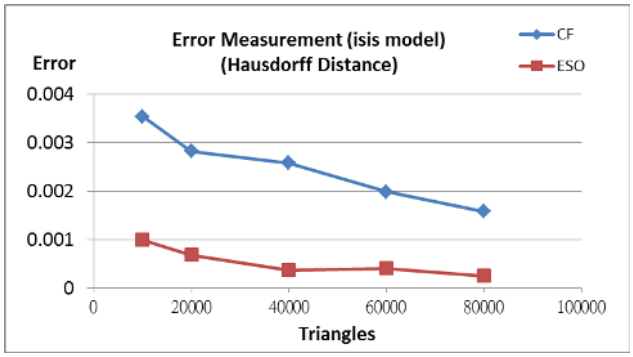

Fig. 17: Error measurement for isis model

In terms of feature preservation, Fig. 18 shows the comparison results of the QEM, the CF and the proposed method for simplifying the cow model into one with 580 triangles. Apparently, regarding the cow horn features, the CF can preserve the model features better than the QEM. However, the former also impact on the outline of cow neck. The proposed method can not only preserve the outline of cow horn, but also retain the shape of cow neck. In addition, Fig. 19 shows the comparison results of the CF and the proposed method for simplifying the dragon model into one with 5076 triangles. The figure shows that our method can retain more teeth and eye features of the dragon model than the CF.

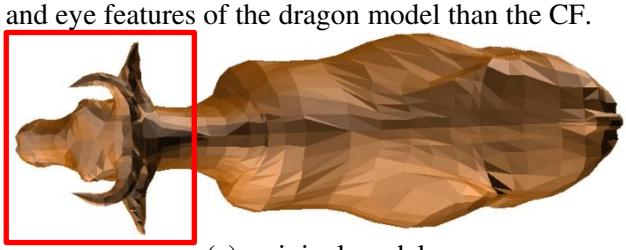

(a) original model

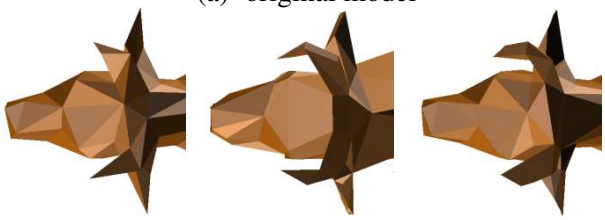

(b) QEM (c) CF (d) ESO

Fig. 18: Comparison of the features of cow horns and neck (580 triangles).

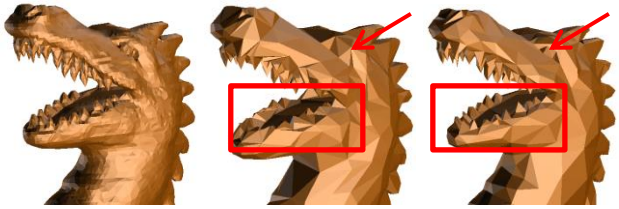

(a) original model (b) CF (c) ESO

Fig. 19: Comparison of the features of dragon teeth (5076 triangles).

Moreover, the Curvature Factor method will also destroy the features of hole easily due to the improper angle estimation on non-manifold surfaces. Taking the femur model as an example, although the boundary vertices by the hole are not on a high-curvature surface, the triangles meeting these vertices are still destroyed easily due to being taken for on a high-curvature surface.

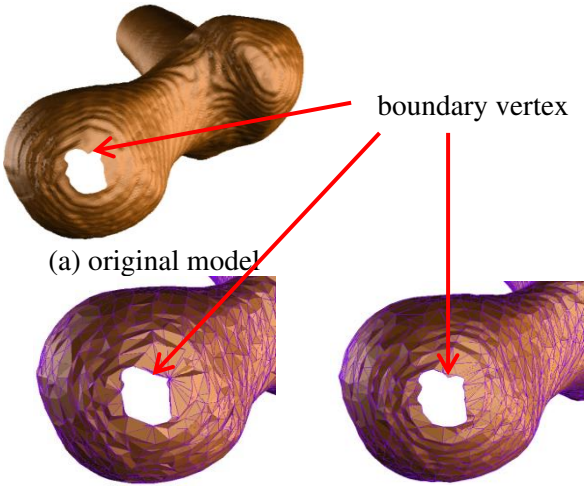

(a) original model

(b) CF (c) ESO

Fig. 20: Comparison of the hole features of femur (7666 triangles).

6 Conclusions

The primary objective of 3D model simplification is to maintain the characteristic contours of the model despite reducing the resolution. The Curvature Factor method employs the Gaussian Curvature to preserve features of simplified models. However, it can only be used to simplify manifold models. To preserve the features of non-manifold model, this study proposes a novel method, called the Extended Shape Operator. The proposed method uses three-rings Shape Operator to estimate the surface variation and preserves more features than the Curvature Factor. Experimental results show that the Extended Shape Operator can also reduce the error caused by simplification.

References:

[1] M. Garland and P. S. Heckbert, Surface simplification using quadric error metrics, *SIGGRAPH 97 Conference Proceedings*, 1997, pp. 209-216.

[2] B. S. Jong, J. L. Tseng, W. H. Yang and T. W. Lin, Extracting Features and Simplifying Surfaces using Shape Operator, *International Conference on Information, Communications and Signal Processing*, 2005, pp.1025-1029.

[3] J. L. Tseng, Shape-based simplification for 3d animation models using shape operator sequences, *4th NAUN/WSEAS International Conference on Communications and Information Technology*, Corfu Island, Greece, July 22-25, 2010, pp.90-95.

[4] P. F. Lee and C. P. Huang , The DSO Feature Based Point Cloud Simplification, *2011 Eighth International Conference on Computer Graphics, Imaging and Visualization*, 2011, pp.1-6.

[5] Z. Y. Yang, S. W. Xu and W. Y. Wu, A Mesh Simplification Algorithm for Keeping Local Features with Mesh Segmentation, *2010 International Conference on Mechanic Automation and Control Engineering*, 2010, pp.5487-5490.

[6] Y. Li, Q. Zhu, A New Mesh Simplification Algorithm Based on Quadric Error Metrics, *International Conference on Advanced Computer Theory and Engineering*, 2008, pp.528-532.

[7] A. Gu´eziec, Surface simplification with variable tolerance, *Second Annual Intl. Symp. on Medical Robotics and Computer Assisted Surgery (MRCAS '95)*, 1995, pp.132–139.

[8] H. Bernd , A Data Reduction Scheme for Triangulated Surfaces, *Computer Aided Geometric Design*, Vol.11, 1994, pp.197-214.

[9] J. Rossignac and P. Borrel , Multi- resolution 3D approximations for rendering complex scenes , *Modeling in Computer Graphics: Methods and Applications*, 1993, pp. 455–465.

[10] T. S. Gieng, B. Hamann, K. I. Joy, Gregory L. Schussman, and Issac J. Trotts, Constructing hierarchies for triangle meshes , *IEEE Transactions on Visualization and Computer Graphics* vol.4, no.2 , 1998, pp.145–161.

[11] P. Cignoni, C. Rocchini, R. Scopigno, Metro: measuring error on simplified surfaces, *Computer Graphics Forum*, Vol.17, No.2, 1998, pp.167-174.

[12] V. Ungvichian and P. Kanongchaiyos, Mesh Simplification Method Using Principal Curvatures and Directions, *Computer Modeling in Engineering & Sciences*, Vol.77, No.4, 2011, pp.201-220.

[13] B. S. Jong, J. L. Tseng and W. H. Yang, An Efficient and Low-Error Mesh Simplification Method Based on Torsion Detection, *The Visual Computer*, Vol.22, No.1, Jan. 2006, pp.56-67.

[14] T. Zhanhong and Y. Shutian, A Mesh Simplification Algorithm Based on Curvature Factor of Collapsing Edge, *2nd IEEE International Workshop on Database Technology and Applications*, 2010, pp.1-3.

[15] M. H. Mousa and M. K. Hussein, Adaptive visualization of 3D meshes using localized triangular strips, *WSEAS Transactions on Computers*, Vol.11, No.4, 2012, pp.101-110.

[16] H. U. Khan, Replica Technique for Geometric Modelling, *WSEAS Transactions on Information Science and Applications*, Vol.6, No.6, 2009, pp.1071-1081.

[17] C. D. Ruberto, M. Gaviano, A. Morgera, Shape Matching by Curve Modelling and Alignment, *WSEAS Transactions on Information Science and Applications*, Vol.6, No.4, 2009, pp.567-578.

[18] M. Chena, B. Tub, B. Lu, Triangulated manifold meshing method preserving molecular surface topology, *Journal of Molecular Graphics and Modelling*, Vol.38, 2012, pp. 411-418.

[19] M. Meyer, M. Desbrun, P. Schröder , A.H. Barr, Discrete Differential-Geometry Operators for Triangulated 2-Manifolds, *Proceedings of VisMath*, 2002.

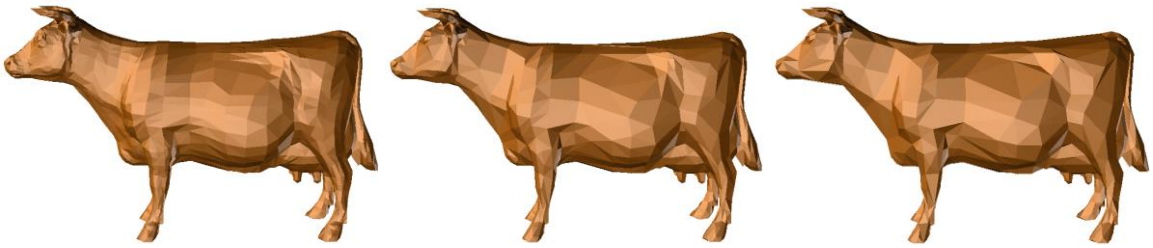

(a) 5804 triangles (original model) (b) 2321 triangles (40%) (c) 1741 triangles (30%)

(d) 1160 triangles (20%) (e) 580 triangles (10%) (f) 290 triangles (5%)

Fig. 21: Simplification results of the cow model using the ESO.

(a) 50761 triangles (original model) (b) 20304 triangles (40%) (c) 15228 triangles (30%)

(d) 10152 triangles (20%) (e) 5076 triangles (10%) (f) 2538 triangles (5%)

Fig. 22: Simplification results of the dragon model using the ESO.

(a) (b) (c) (d) (e) (f)

Fig. 23: Simplification results of the femur model using the ESO. (a) 153322 triangles (original model), (b) 61328 triangles, (c) 45996 triangles, (d) 30664 triangles, (e) 15332 triangles, (f) 7666 triangles.

(a) (b) (c) (d) (e) (f)

Fig. 24: Simplification results of the isis model using the ESO. (a) 200000 triangles (original model), (b) 80000 triangles, (c) 60000 triangles, (d) 40000 triangles, (e) 20000 triangles, (f) 10000 triangles.